Experimental Neurology 233 (2012) 463–471

Contents lists available at SciVerse ScienceDirect

Experimental Neurology

journal homepage: www.elsevier.com/locate/yexnr

Regular Article

Widespread suppression of huntingtin with convection-enhanced delivery of siRNA

David K. Stiles [a], Zhiming Zhang [b], Pei Ge [c], Brian Nelson [a], Richard Grondin [b], Yi Ai [b], Peter Hardy [b], Peter T. Nelson [d], Andrei P. Guzaev [e], Mark T. Butt [f], Klaus Charisse [c], Verbena Kosovrasti [c], Lubomir Tchangov [c], Michael Meys [c], Martin Maier [c], Lubomir Nechev [c], Muthiah Manoharan [c], William F. Kaemmerer [a], Douglas Gwost [a], Gregory R. Stewart [a], Don M. Gash [b], Dinah W.Y. Sah [c,*]

[a] Medtronic Neuromodulation, Medtronic, Minneapolis, MN 55432, USA
[b] Department of Anatomy and Neurobiology, University of Kentucky College of Medicine, Lexington, KY 40536, USA
[c] Alnylam Pharmaceuticals Inc., Cambridge, MA 02142, USA
[d] Sanders Brown Center on Aging, University of Kentucky College of Medicine, Lexington, KY 40536, USA
[e] AM Chemicals LLC, Oceanside, CA 92056, USA
[f] Tox Path Specialists, LLC, Walkersville, MD 21793, USA

ARTICLE INFO

Article history:
Received 24 June 2011
Revised 3 November 2011
Accepted 10 November 2011
Available online 19 November 2011

Keywords:
Huntington's disease
Site-specific delivery
Convection enhanced delivery
Putamen
Striatum

ABSTRACT

Huntington's disease is an autosomal dominant neurodegenerative disease caused by a toxic gain of function mutation in the huntingtin gene (Htt). Silencing of Htt with RNA interference using direct CNS delivery in rodent models of Huntington's disease has been shown to reduce pathology and promote neuronal recovery. A key translational step for this approach is extension to the larger non-human primate brain, achieving sufficient distribution of small interfering RNA targeting Htt (siHtt) and levels of Htt suppression that may have therapeutic benefit. We evaluated the potential for convection enhanced delivery (CED) of siHtt to provide widespread and robust suppression of Htt in nonhuman primates. siHtt was infused continuously for 7 or 28 days into the nonhuman primate putamen to analyze effects of infusion rate and drug concentration on the volume of effective suppression. Distribution of radiolabeled siHtt and Htt suppression were quantified by autoradiography and PCR, respectively, in tissue punches. Histopathology was evaluated and Htt suppression was also visualized in animals treated for 28 days. Seven days of CED led to widespread distribution of siHtt and significant Htt silencing throughout the nonhuman primate striatum in an infusion rate and dose dependent manner. Htt suppression at therapeutic dose levels was well tolerated by the brain. A model developed from these results predicts that continuous CED of siHtt can achieve significant coverage of the striatum of Huntington's disease patients. These findings suggest that this approach may provide an important therapeutic strategy for treating Huntington's disease.

Introduction

Huntington's disease is caused by an autosomal dominant mutation consisting of an expansion in the CAG repeat region in the huntingtin (Htt) gene (The Huntington's Disease Collaborative Research Group, 1993), with 36 or more repeats conferring a gain of functional toxicity (Walker, 2007). The resulting underlying pathology is characterized by atrophy of the striatum, including profound degeneration of medium spiny neurons, as well as atrophy of the cortex and other regions of the brain. Clinical manifestations include progressive involuntary movement, cognitive dysfunction and behavioral changes. Currently, there are no therapies that modify the underlying progression of disease.

RNA interference (RNAi) is a naturally occurring cellular mechanism of gene regulation that can be leveraged for selectively suppressing Htt expression. Studies in rodent models of Huntington's disease have demonstrated the clinical potential of Htt lowering strategies using RNAi for reducing neuropathology, improving motor behavior and extending survival time (Boudreau et al., 2009; DiFiglia et al., 2007; Drouet et al., 2009). Because of the blood–brain barrier, one of the major challenges in translating RNAi treatments into clinical treatments for neurodegenerative diseases is delivery. Theoretically, convection enhanced delivery (CED) which entails infusing molecules under positive pressure to increase the volume of distribution in target tissues should be an effective means for delivering small interfering RNA (siRNA) targeting Htt into selected brain sites. The term "convection" in the context of CED refers to bulk flow in tissue that occurs as a result of pressure gradients, which greatly enhances the distribution of both small and large molecules

Abbreviations: (CED), convection enhanced delivery; (c_{inf}), concentration of infused siRNA; (c_s), threshold tissue concentration for suppression; (Htt), huntingtin; (Q), infusion rate; (RNAi), RNA interference; (siRNA), small interfering RNA; (V_s), volume of suppression; ($V_{s,Str}$), volume of suppression within the striatum.

* Corresponding author at: Alnylam Pharmaceuticals Inc., 300 Third Street, Cambridge, MA 02142, USA. Fax: +1 617 551 8102.
E-mail address: dsah@alnylam.com (D.W.Y. Sah).

0014-4886/$ – see front matter © 2011 Elsevier Inc. All rights reserved.
doi:10.1016/j.expneurol.2011.11.020

(Bobo et al., 1994). CED can occur with either acute or chronic infusion dosing paradigms of molecules, at increasing or constant flow rates; the molecules are "carried" by the movement of the effluent through the interstitium. This method has been used successfully for delivering molecules in the siRNA size range into the brain in animals and humans, resulting in far greater distribution than possible by passive diffusion (Bobo et al., 1994; Fiandaca et al., 2009; Song and Lonser, 2008). Clinical precedent for direct delivery of drugs into the brain with CED includes ~3 hour infusion at 0.5–10 μL/min of glucocerebrosidase in a Gaucher's patient (Lonser et al., 2007), and continuous infusion of Trabedersen for up to 22 weeks at 1 and 4 μL/min in patients with glioblastoma or anaplastic astrocytoma (Bogdahn et al., 2011).

Here, 7 days of CED of a radiolabeled siRNA (^{14}C-siHtt) targeting both wild type and mutant Htt was used to evaluate siRNA distribution and Htt suppression after infusion into the non human primate putamen. The study was designed to enable development of an empirical model of the Volume of Suppression (V_s) by choosing concentrations of siRNA and infusion rates that span a range of clinically relevant steady-state dosing regimens. Seven days of CED led to widespread distribution of siRNA and silencing of Htt mRNA and protein. These data were then used to model the dependence of the volume of effective suppression (volume over which effective siRNA concentrations are attained) on infusion rate and concentration of siRNA. In addition, a second study was conducted to analyze histopathology following 28 days of continuous CED in the putamen to assess brain tissue responses to silencing Htt mRNA and lowering protein levels. Collectively, the results show that 7 or 28 days of CED of siRNA leads to widespread and robust suppression of Htt which is well tolerated in the nonhuman primate brain. The results support the clinical potential of this approach for the treatment of Huntington's disease.

Materials and methods

Animal surgery and siRNA delivery

All animal procedures were approved by the Animal Care and Use Committee of the University of Kentucky, which is accredited by the Association for Assessment and Accreditation of Laboratory Animal Care. Female rhesus monkeys (*Macaca mulatta*), approximately 7–16 years old, weighing 4.4–8.1 kg were obtained from Covance Research Products (Alice, Texas). MRI-guided stereotaxic surgery (Grondin et al., 2001; Heiss et al., 2010) was conducted to implant an intraparenchymal catheter with a titanium needle tip into the right putamen. The catheter was connected to a SynchroMed® II Pump (Medtronic Neurological, Minneapolis, MN) subcutaneously implanted in the abdomen. After a 7 day infusion of phosphate buffered saline at 6 μL/day, pumps were re-filled with test article and programmed for continuous delivery for 7 days. The conditions chosen for this experiment (Table 1 plus phosphate buffered saline group, 0.3 μL/min, n = 5) were designed to optimize modeling distribution at varying flow rates and drug concentrations. At the end of test article infusion, animals were euthanized using American Veterinary Medical Association approved methods. Tissue was evaluated from animals that met pre-determined criteria of accurate catheter placement and patency. The first criterion comprised catheter tip placement of ≤2 mm radial distance from the intended target position, as determined by post-operative MRI; for this study, all nonhuman primates implanted met this criterion. The second criterion comprised catheter patency as determined by post-necropsy quantitative autoradiography (qAR) evaluation of brain tissue sections (see below); if no qAR signal was present, then this nonhuman primate was not included for further analysis. The catheter patency criterion was not met in only one animal (from the 0.5 μL/min, 4 mg/mL group) in this study.

Table 1
Amount of siRNA infused per day (mg/d) and corresponding relative (%) Htt/GAPDH mRNA suppression obtained in putamenal tissues punches, at different infusion rates and concentrations of siRNA infused.

		Infusion Rate (μL/min)		
		0.1	0.3	0.5
Concentration of siRNA Infused (mg/mL)	16	2.30 mg/d 28% N = 3		11.52 mg/d 42% N = 3
	12		5.18 mg/d 44% N = 5	
	8		3.46 mg/d 39% N = 5	
	4	0.58 mg/d 16% N = 3		2.9 mg/d 16% N = 2

siRNA

The radiolabeled siRNA (Supplemental Fig. 1 online) was synthesized and purified according to standard procedures with minor modifications as follows. A deoxythymidine phosphoramidite building block, ^{14}C-labeled at C-4, was synthesized and coupled to a solid support-bound, protected oligonucleotide precursor followed by deprotection and anion-exchange HPLC purification of the radiolabeled antisense strand. The radiolabeled antisense strand was then annealed to the unlabeled sense strand, and diluted in PBS. The silencing activity of this modified siRNA was found to be unchanged compared to the parent unlabeled siRNA. The final specific activity of the ^{14}C-siHtt was 2.0 μCi/mg, and osmolarity and endotoxin levels were confirmed to be within acceptable levels.

Htt mRNA quantitation

For each animal, the infusion point in the brain was identified with MRI and visual inspection of the 2 mm coronal brain sections at necropsy, prior to storage at −80 °C. After partial thawing on ice, tissue punches of 1.2 mm diameter were taken using a pre-defined punch template (Supplemental Fig. 2), and stored at −80 °C prior to blinded analysis for Htt and GAPDH mRNA by RT-qPCR at QPS Pharmaceutical Services, using standard methods. To normalize data across plates, a "common control" derived from naïve rhesus monkey brain tissue was included on each RT-qPCR plate. The qPCR data were unblinded after all data were obtained.

Western blot analysis

Additional tissue punches, located 4 mm from the infusion site, were used for Western blot analysis with mouse anti-Huntingtin (MAB2166, Millipore, Billerica, MA) and rabbit anti-β-catenin (Abcam, Cambridge, MA) primary antibodies, followed by fluorescently-labeled secondary antibodies (anti-rabbit 680 nm and anti-mouse 800 nm, LI-COR Bioscience) for detection. Standard curves were generated from pooled striatal tissue samples from phosphate buffered saline-treated animals, using 5, 10 or 15 μg protein per lane. For test samples, 15 μg protein per lane was evaluated for a tissue punch located within the putamen from each of 3 animals from the 12 mg/mL ^{14}C-siHtt and control groups, after 7 days of infusion at 0.3 μL/min.

Determination of tissue concentration of ^{14}C-siHtt

Photographs were obtained of the 2 mm coronal brain sections after 40 μm thick coronal sections and tissue punches had been taken for quantitative autoradiography (qAR) imaging and RT-qPCR processing, respectively. The spatial location of the punches was determined by calibrating the image files to a known length scale and compared to the qAR image. The ^{14}C-siHtt concentration at the

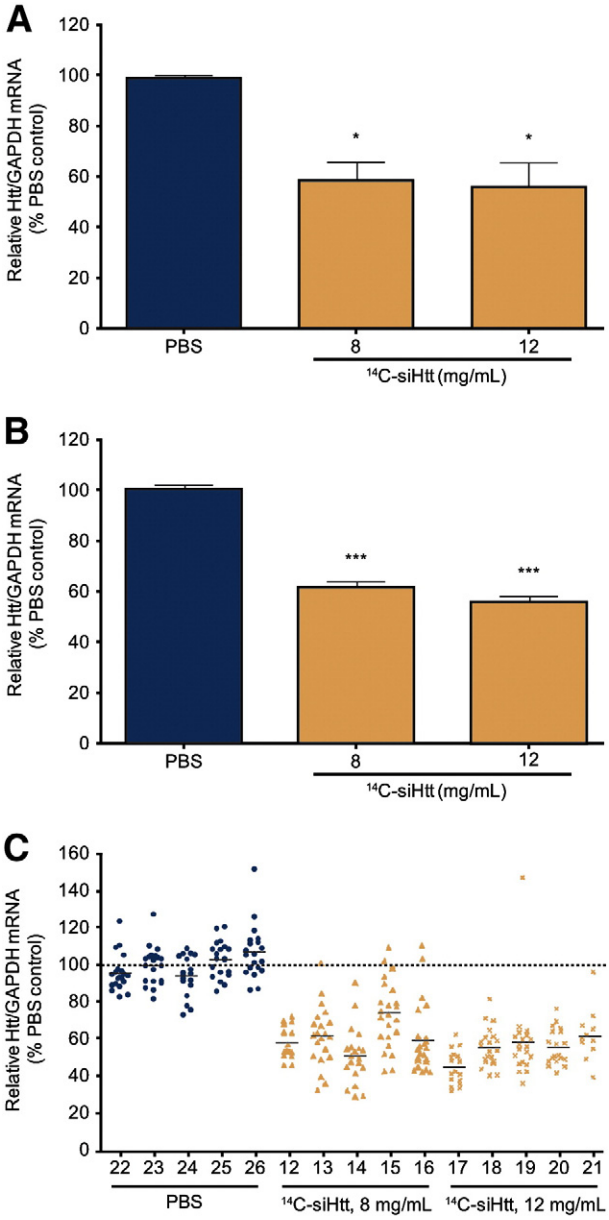

Fig. 1. Htt/GAPDH mRNA suppression in tissue punches from the 8 and 12 mg/mL ^{14}C-siHtt groups, compared to PBS control (n = 5/group), after 7 days of infusion at 0.3 μL/min. Tissue punches located within the putamen at a distance of 0 to 2 mm (A) or 4 mm (B) from the infusion site were evaluated for Htt/GAPDH mRNA. *p<0.05 and ***p<0.001 by one-way ANOVA with Tukey's post-hoc test versus the PBS group. Panel C shows the relative level of Htt/GAPDH mRNA in all individual tissue punches located 4 mm from the infusion site for each animal. Error bars represent SEM.

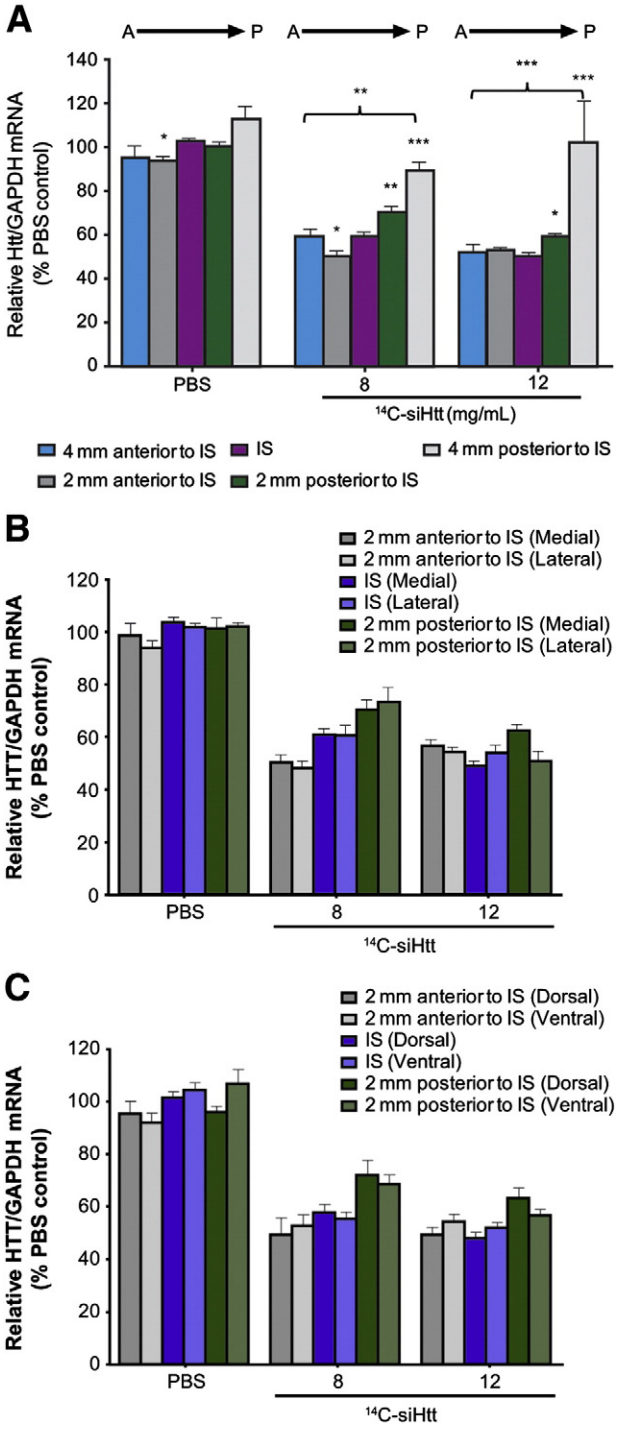

Fig. 2. The anterior–posterior (A), medial–lateral (B) and dorsal–ventral (C) dependences of Htt mRNA suppression are shown in tissue punches located 4 mm from the infusion site. For anterior–posterior dependence of Htt mRNA suppression, data are presented by group, from tissue sections (in left to right order) 4 mm and 2 mm anterior to the infusion site, at the infusion site, and 2 mm and 4 mm posterior to the infusion site. *p<0.05, **p<0.01 and ***p<0.001 by two-way ANOVA with Bonferroni post-hoc test versus the section at the infusion site. For medial–lateral and dorsal–ventral dependences of Htt mRNA suppression, there were no significant differences as assessed by two-way ANOVA with Bonferroni post-hoc test versus the section at the infusion site. Error bars represent SEM.

punch location was then calculated using MCID™ v7.0 imaging analysis software (InterFocus Imaging, Cambridge, United Kingdom), assuming that no ^{14}C-siHtt degradation had occurred.

Histopathology

Using the same delivery system and following the same surgical procedures for the distribution and suppression study, ten additional animals received either vehicle (n = 5) or 8 mg/mL unlabeled Htt siRNA (n = 5) infused into the putamen at the rate of 0.3 μL/min for 28 days. Using histopathological and immunohistochemical methods described elsewhere (Ai et al., 2003), microscopic evaluations were conducted on 40 μm thick coronal brain sections from the rostral striatum through to the brain stem. Sections were stained with Hematoxylin and Eosin, Nissl, or Fluoro-Jade B. Immunostaining for Htt, GFAP or HLA-DR was conducted using a rat anti-Htt protein (549–679) monoclonal antibody (MAB2174, Millipore, Billerica,

MA), a mouse anti-GFAP monoclonal antibody (MAB360, Chemicon, Temecula, CA), or a mouse anti-HLA-DR monoclonal antibody (Clone L243, BD Biosciences, San Jose, CA), respectively.

Calculation of V_s and determination of empirical function for V_s (Q, c_{inf})

The V_s in each nonhuman primate was obtained by spatially orienting the autoradiographic images in Amira® v5.2.0 (Visage Imaging, Inc., San Diego, CA). Using the known spacing between each coronal brain section and the pixel size calibrated using MCID, the pixel volume was calculated. All pixels with concentrations greater than c_e were then summed to determine V_s. The response model determining the empirical function for V_s as a function of infusion rate (Q) and the concentration of the infused siRNA (c_{inf}) was generated using Design-Expert® (v. 8.0.1, Stat-Ease, Inc., Minneapolis, MN).

Statistics

To determine the significance of Htt mRNA suppression versus a control or reference condition, one-way or two-way ANOVA with Tukey's or Bonferroni post-hoc test was used. For Figs. 1A and B, one-way ANOVAs were used for statistical analysis because the study was intended to address 2 separate questions: 1) how the response (Htt mRNA reduction) was affected by dose near the infusion site (i.e. at a 0–2 mm radial distance from the infusion site) after siRNA treatment, in order to demonstrate siRNA activity in NHP, and 2) how the response (Htt mRNA reduction) was affected by dose at a 4 mm radial distance from the infusion site after siRNA treatment, in order to demonstrate significant siRNA activity at a distance consistent with CED. In addition, all punches at either a 0–2 mm or 4 mm radial distance from the infusion site, irrespective of anatomical location within the putamen, were grouped together for the analysis, rather than comparing each treatment sample to its anatomical counterpart in the PBS group. We did not have a large enough sample size with the current data set to be able to resolve the data analysis at this level, with a number of punch locations having 2 or fewer data points for at least one treatment group. The lower confidence interval of the suppression of Htt mRNA in the punches used to calculate c_e, was determined using the T distribution (Minitab, Inc., State College, PA).

Results

CED of siRNA suppresses Htt mRNA throughout the striatum and lowers Htt protein levels

Previous studies have demonstrated silencing of Htt throughout the rat striatum with intrastriatal infusion of siRNA targeting Htt (Ge et al., 2009). Here, the translational potential of direct CNS delivery of siRNA for silencing Htt was evaluated in the significantly larger nonhuman primate striatum, a critical step in developing this potential therapy for Huntington's disease. This study tested varying infusion rates (0.1, 0.3 and 0.5 μL/min) and siRNA concentrations (4, 8, 12, and 16 mg/mL), with Htt mRNA suppression measured for all test conditions. The boundary conditions were based on preliminary experiments suggesting that they represented appropriate limits for the study. The center point conditions of 0.3 μL/min infusion rate and either 8 or 12 mg/mL siRNA concentration were used as the main independent variable conditions for which to study the effects on Htt mRNA suppression. From preliminary experiments, 7 days was found to be a sufficient period of time for siRNA delivery to reach steady state; thus, the results of this study represent the extent of Htt suppression achievable under these delivery conditions. The siRNA was radiolabeled (^{14}C-siHtt) to facilitate correlation of Htt silencing with spatial distribution of siRNA within the same animal (see below). In vitro studies had demonstrated that radiolabeling had no effect on Htt suppression with the siRNA sequence used in these experiments (data not shown). Silencing of Htt mRNA was assessed in tissue punches taken from specific locations in the putamen and caudate using a template placed over 2 mm thick serial coronal sections of the brain, extending 6 mm anterior to 6 mm posterior from the infusion site (Supplemental Fig. 2 online). In addition, suppression of Htt protein was evaluated by semi-quantitative Western blot analysis using tissue punches from the putamen.

For all tested combinations of infusion rate and ^{14}C-siHtt concentration, significant (15.5 to 44.4%) reduction of Htt mRNA was observed throughout the putamen and caudate relative to vehicle infusion. Suppression of mRNA was dose-dependent for a given infusion rate. For the boundary conditions (4 or 16 mg/mL ^{14}C-siHtt at 0.1 or 0.5 μL/min), Htt mRNA suppression in the putamen was more pronounced with increased siRNA concentration than with increased infusion rate (Table 1), although both variables and their interaction are important in the response model that was developed from these data (see below). Of particular interest were the center point conditions of 8 and 12 mg/mL at 0.3 μL/min, where more extensive spatial analysis was performed. For both groups, there was statistically significant reduction of Htt mRNA of approximately 40–45% (Table 1). The level of Htt mRNA suppression in the putamen at a 0 to 2 mm distance from the infusion site (Fig. 1A) was similar to that at 4 mm from the infusion site (Fig. 1B), consistent with the principle of CED that drug is distributed more uniformly with positive pressure than with diffusion which results in exponential decline of drug concentration with distance from the infusion site (Groothuis et al., 1999). Consistent Htt mRNA reduction was obtained across animals within the same treatment group with low variability across punches from the same animal (Fig. 1C).

To assess directional dependence, Htt mRNA suppression in tissue punches at an approximately 4 mm distance from the infusion site was evaluated along each axis: anterior–posterior (Fig. 2A), medial–lateral (Fig. 2B) and dorsal–ventral (Fig. 2C). While there was substantial suppression of Htt mRNA throughout almost all of the putamen after 7 days of infusion of 8 or 12 mg/mL ^{14}C-siHtt, punches taken from locations 4 mm posterior to the infusion site showed significantly less suppression on average than those taken from coronal sections at or anterior to the infusion site (Fig. 2A). In the coronal section 4 mm posterior to the infusion site, the reduction in Htt mRNA was only 21% ($p<0.05$ vs PBS) at 8 mg/mL, and the reduction obtained using 12 mg/mL ^{14}C-siHtt was not significantly different from vehicle controls. In contrast, in the coronal section 4 mm anterior to the infusion site, there was a substantial 38% and 45% reduction of Htt mRNA with 8 and 12 mg/mL ^{14}C-siHtt, respectively, relative to the corresponding vehicle group, that was significantly different ($p<0.01$ and $p<0.001$, respectively) from the coronal section 4 mm posterior to the infusion site.

Htt mRNA suppression in tissue punches within the putamen was consistent across the medial–lateral (Fig. 2B) and dorsal–ventral (Fig. 2C) axis. Significant reduction of Htt mRNA extended into the adjacent caudate with intraputamenal infusion. CED of 8 or 12 mg/mL ^{14}C-siHtt at 0.3 μL/min resulted in 17% or 19% suppression of Htt mRNA, respectively ($p<0.01$ or $p<0.001$ versus vehicle control group), in the caudate.

Suppression of Htt protein in tissue punches from the putamen, as assessed by semi-quantitative Western blot analysis, corresponded qualitatively to mRNA changes (data not shown). CED of 12 mg/mL ^{14}C-siHtt at 0.3 μL/min resulted in a reduction of Htt protein by 32% on average compared with a 44% average reduction of Htt mRNA, relative to the vehicle control group.

Correlation of siHtt tissue concentration with Htt mRNA suppression and determination of threshold tissue concentration for suppression

To correlate tissue concentration of siRNA with extent of Htt mRNA suppression, quantitative autoradiographic determinations of ^{14}C-siHtt concentration in coronal brain sections were co-registered

with tissue punch locations (Fig. 3A). Radioactivity counts were assumed to represent parent ^{14}C-siHtt; this is a conservative assumption for calculating the threshold ^{14}C-siHtt tissue concentration needed for a certain level of Htt mRNA suppression. These data, from 422 tissue punches from putamen and caudate, are shown in Fig. 3B. From RNAi studies reported to-date in animal models of Huntington's disease, Htt mRNA suppression of approximately 45% or greater has resulted in meaningful normalization of neuropathology and behavior (Harper et al., 2005). The subset of tissue punches in this study that demonstrated at least 45% reduction of Htt mRNA, was therefore considered to have siRNA concentrations that are equal to or greater than the threshold suppression concentration, c_s. In these 244 tissue punches from the striatum, the measured c_s of ^{14}C-siHtt was 0.65 mg_{siHtt}/g_{tissue} which corresponded to an average Htt mRNA suppression of 46.1% with a 90% lower confidence interval of 45.1%.

As described above, there was directionality to mRNA suppression within the putamen along the anterior–posterior axis, with punches from the coronal section located 4 mm posterior to the infusion site exhibiting significantly less Htt silencing. To assess whether tissue concentrations of siRNA were also lower in this location, levels of ^{14}C-siHtt were determined. In the 8 mg/mL ^{14}C-siHtt group, punches taken from the section located 4 mm posterior to the infusion site exhibited significantly lower levels of ^{14}C-siHtt than those from the section located 4 mm anterior to the infusion site (0.25 mg/g versus 1.54 mg/g, respectively, $p = 0.029$), consistent with the reduced effect on mRNA suppression (21 vs 38% suppression, respectively, $p < 0.01$).

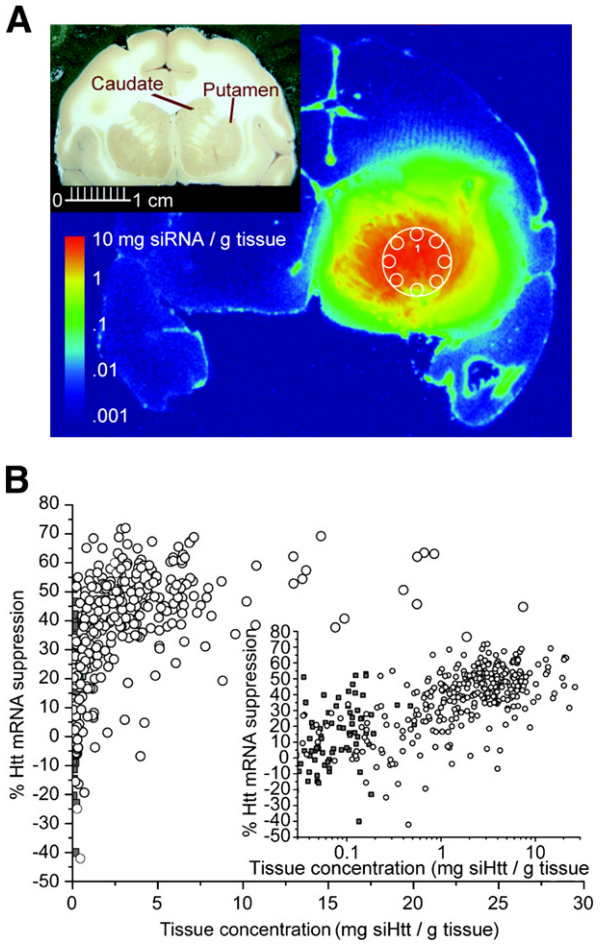

Fig. 3. Tissue concentrations of ^{14}C-siHtt and correlation with suppression of Htt mRNA. Panel A is a heat map representation of quantitative autoradiography of a coronal section encompassing the infusion site after 7 days of 12 mg/mL ^{14}C-siHtt infusion at 0.3 μL/min. The logarithmic color scale indicates the concentration of ^{14}C-siHtt in the tissue. The white circles represent the locations of tissue punches taken for mRNA quantitation. The inset comprises a photograph of a corresponding coronal brain section with the caudate and putamen labeled. The calibration bar is 1 cm in length, with mm subdivisions. Panel B shows the correlation of percent Htt/GAPDH mRNA suppression, relative to PBS control, with tissue concentration of ^{14}C-siHtt from individual tissue punches taken from all animals in the study. Inset: the same data is shown with the tissue concentration plotted on a semi-logarithmic scale. Open and filled squares represent data from tissue punches taken from putamen and caudate, respectively.

Volume of suppression — dependence on concentration of siRNA infused and infusion rate

For local drug delivery to the CNS, it is critical to ensure that sufficient drug distribution in the brain is achieved for the intended therapeutic effect. The *volume of suppression*, V_s, is defined as the region in the brain where the siRNA has a meaningful biological effect; every point in this volume has a tissue concentration equal to or greater than the target *threshold tissue concentration for suppression*, c_s. Two key factors that impact V_s (mm^3) are infusion rate (Q, μL/min) and concentration of drug infused (c_{inf}, mg/mL). In the present study, V_s, as measured by quantitative autoradiography, increased with increasing infusion rates, or with increasing concentrations of siRNA infused (Table 2). With 4 or 16 mg/mL ^{14}C-siHtt, an infusion rate of 0.5 μL/min resulted in a larger V_s in the brain and striatum, compared with an infusion rate of 0.1 μL/min. A ^{14}C-siHtt concentration of 16 mg/mL resulted in a larger V_s in the brain and striatum, compared with 4 mg/mL ^{14}C-siHtt, whether at an infusion rate of 0.1 or 0.5 μL/min. At an infusion rate of 0.3 μL/min, a ^{14}C-siHtt concentration of 12 mg/mL resulted in a larger V_s in the brain and striatum, compared with 8 mg/mL ^{14}C-siHtt.

Table 2
Measured V_s (brain) and $V_{s,\,Str}$ (striatum) in individual NHPs at different infusion rates (Q) and concentrations of siRNA infused (c_{inf}) for ≥45% suppression.

Monkey no.	Infusion rate (μL/min)	Concentration (mg/mL)	V_s (mm^3)	$V_{s,\,Str}$ (mm^3)
1	0.1	4	232.4	13.7
2	0.1	4	75.2	28.1
3	0.1	4	156.6	156.6
		Mean volume ± SEM	154.7 ± 45.3	66 ± 45.4
4	0.1	16	1160.8	539.2
5	0.1	16	936.6	555.5
6	0.1	16	519	454.3
		Mean volume ± SEM	872.1 ± 188.1	516.3 ± 31.4
7	0.5	4	748.1	188
8	0.5	4	655.4	309.3
		Mean volume ± SEM	701.8	248.7
9	0.5	16	3819.2	1543.8
10	0.5	16	2468.4	1182.1
11	0.5	16	3515.5	1058.9
		Mean volume ± SEM	3267.7 ± 409.2	1261.6 ± 145.5
12	0.3	8	563.2	506.5
13	0.3	8	987.2	348.1
14	0.3	8	781.2	530.9
15	0.3	8	720.2	302.8
16	0.3	8	812.1	667.9
		Mean volume ± SEM	772.8 ± 68.7	471.2 ± 66.0
17	0.3	12	1813.5	1110.6
18	0.3	12	1961.3	1240.7
19	0.3	12	922.5	470.4
20	0.3	12	820.6	740.9
21	0.3	12	1468.2	779.3
		Mean volume ± SEM	1397.2 ± 229.6	868.4 ± 137.8

For a target c_s corresponding to 45% Htt mRNA suppression, and the obtained V_s measured from quantitative autoradiography data for a given infusion rate Q and concentration of drug infused c_{inf} (Table 2), a response surface model describing V_s as a function of Q and c_{inf} was generated. A regression analysis was performed to curve-fit the data with a second order polynomial function of the form: $V_s(Q,c_{inf}) = a_0 + a_1Q + a_2c_{inf} + a_3Qc_{inf} + a_4Q^2 + a_5c_{inf}^2$ (1). For this experiment, the curvature was not found to be statistically significant within the ranges tested, so only the terms a_1, a_2 and a_3 were used in the regression model for V_s. The empirical function obtained for V_s (adjusted R^2 of 0.85) demonstrates a linear dependence on Q and c_{inf} as well as the interaction term Qc_{inf}.: $V_s(Q,c_{inf}) = -139.0 - 304.7Q + 21.9c_{inf} + 393.4Qc_{inf}$ (2). With this response model, it is possible to estimate the V_s as a function of any value of Q and c_{inf} within the experimentally-tested design space (Fig. 4).

In addition, V_s observed in the striatum only ($V_{s,\,Str}$) was measured (Table 2), and with c_s corresponding to 45% Htt mRNA suppression, the resultant empirical function (adjusted R^2 of 0.69) demonstrates a linear dependence on Q and c_{inf} only, with the interaction term Qc_{inf} being negligible: $V_{s,\,Str}(Q,c_{inf}) = -389.0 + 1258.2Q + 61.2c_{inf}$ (3).

Histopathology

Infusion of vehicle and siRNA for 28 days was well tolerated; no behavioral changes were observed and tissue responses to catheter implantation and CED infusion were restricted to the catheter track and adjacent tissue in the putamen. Changes in tissue adjacent to the catheter track in both vehicle and siRNA recipients included some circumscribed neuronal loss, mild astrocytosis as assessed by an increase in GFAP-immunoreactive cells, and reactive microgliosis, as assessed by an increase in HLA-DR-immunoreactive cells. The circumscribed neuronal loss appeared to be associated with catheter implantation. The relatively high infusion rate may have also contributed to the pathological changes at the injection site. Fluoro-Jade B staining did not reveal any continuing neuronal necrosis, either at the catheter dosing site or in brain regions away from the catheter site, in any of the 28 day control and siRNA treated animals. Decreased neuronal levels of Htt protein were indicated by a pronounced attenuation of immunostaining intensity in the putamen of siRNA recipients, while Nissl-staining was retained (Fig. 5). Decreases in immunostaining were evident for up to 11.5 mm in rostral–caudal extent. In addition to the putamen, the volume of distribution of the siRNA as indicated by immunostaining spread into the adjacent caudate nucleus and nucleus accumbens. Attenuated Htt immunostaining was not seen in vehicle recipients.

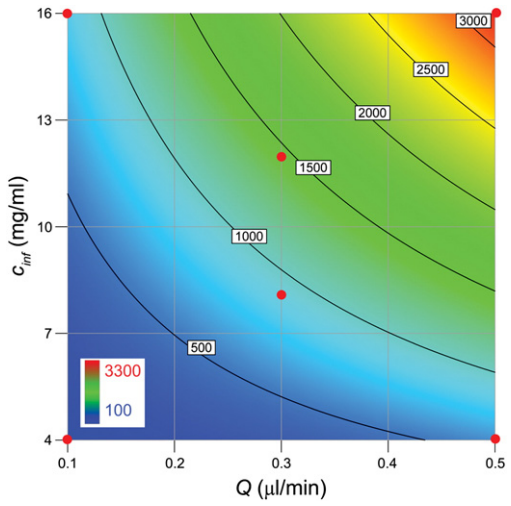

Fig. 4. Color contour plot of the predicted total V_s as a function of infusion rate (Q, µL/min) and concentration of siRNA infused (c_{inf}, mg/mL), for c_s corresponding to 45% suppression. The predicted total V_s (mm^3) is represented as colors from 100 (dark blue, lower left) to 3300 mm^3 (bright red, upper right). V_s isocontours are shown as solid dark lines for 500, 1000, 1500, 2000, 2500 and 3000 mm^3. The boundary and center design points of the experiment are shown as filled red circles.

Discussion

A key remaining challenge for achieving the full therapeutic potential of siRNAs for CNS disorders is in vivo delivery to an area of brain sufficient to obtain a clinically meaningful effect. To date, local delivery of siRNA has yielded limited spatial distribution and silencing in neurons (DiFiglia et al., 2007; Kumar et al., 2007; Thakker et al., 2004). Here, we demonstrate that 7 days of CED of siRNA targeting Htt provides distribution of drug and Htt lowering in a large region of the nonhuman primate brain. Moreover, a response model developed with these data provides a way to scale continuous intraparenchymal CED for delivery of efficacious levels of siRNA throughout sufficiently large regions of the human brain for clinical benefit in CNS disorders such as Huntington's disease.

Acute CED has shown experimental success for intraparenchymal CNS administration of molecules ranging from nanoparticles to proteins (Voges et al., 2003), with distribution throughout regions of the nonhuman primate and human brain that are much larger than achievable with passive diffusion, and good tolerability. An important distinction in the present study is that continuous CED infusion over 7 or 28 days was used, versus the previously reported CED infusion durations of minutes to hours. Consequently, the typical measure of CED performance (Song and Lonser, 2008) – the ratio of volume of distribution to volume of infusion (V_d/V_i) – is not appropriate here since the volume of infusion continues to increase with time, while the measured volume of distribution has reached steady-state. Concentration–distance profiles show approximately constant drug concentrations over substantial distances, beyond which concentrations decline exponentially. In the present study, with the infusion site centered in the putamen, spatial profiles of siRNA concentration demonstrated approximately constant siRNA levels over an 8 mm distance within the putamen in the coronal plane, and substantially lower levels in surrounding tissues with increasing distance from the infusion site. The observed 8 mm distribution of Htt lowering was in the large central region of the roughly football-shaped putamen, representing over 50% of the putamenal volume. Along the anterior–posterior axis, both siRNA level and effect were greater at more anterior locations. Further experimentation would be needed to assess whether factors such as asymmetry of anatomical structures or preferential transport paths may result in directional preference. Nonetheless, the results from the present study suggest that CED into gray matter is an effective delivery method for distributing siRNA in the brain.

Despite the identification of mutant Htt as causal for HD in 1993, there are currently no therapies that impact the underlying progression of disease. With the advent of oligonucleotide approaches to gene suppression, Htt lowering strategies have been used across multiple studies assessing approaches that simultaneously lower wild type and mutant Htt expression (Boudreau et al., 2009; Drouet et al., 2009) and that provide allele-specific silencing of mutant Htt by targeting associated single nucleotide polymorphisms (Lombardi et al., 2009; Pfister et al., 2009). Both general approaches can be effective therapeutic strategies, each with its own relative merits. Short hairpin RNAs and siRNAs targeting wild-type and/or mutant Htt have been evaluated in rodent models of Huntington's disease. Continuous, partial suppression of Htt in adult rodent models is effective in reducing neuropathology, improving motor behavior and prolonging survival (Boudreau et al., 2009; Drouet et al., 2009). Importantly, these studies showed striatal suppression of up to 75% of both wild-type and mutant Htt to be not only efficacious against HD pathology, but also well-tolerated for at least 9 months without overt toxicity or

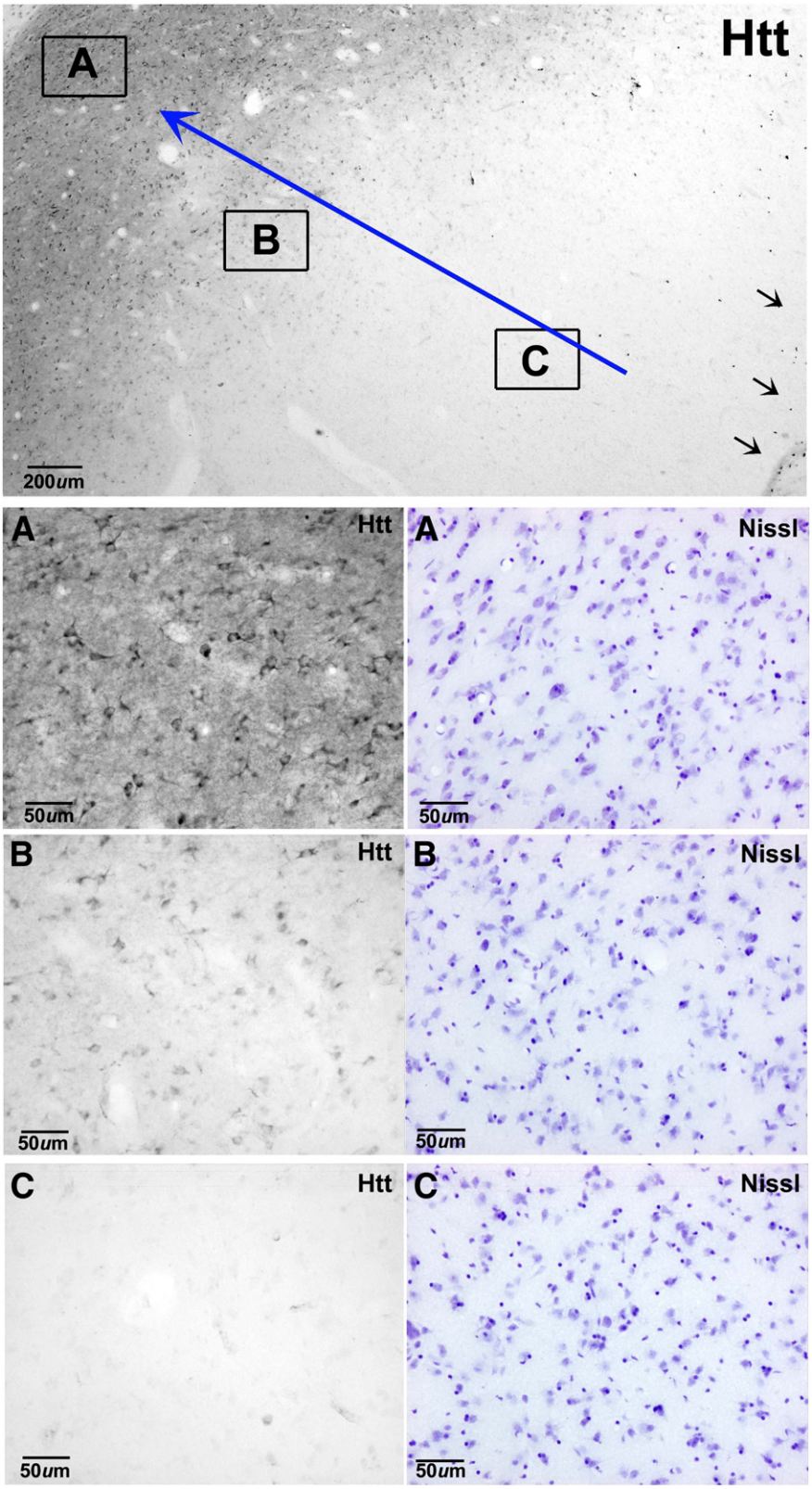

Fig. 5. Normal patterns of Nissl-stained neurons are retained in the putamen while Huntingtin (Htt) immunostaining is suppressed. Htt immunostaining intensity increased with increasing distance from the catheter track (small arrows). A, and insets below: Intense Htt immunostaining of neurons overlapped with normal patterns of Nissl-stained neurons in the putamen beyond the immunostaining penumbra. B, and insets below: In the penumbra, moderately and weakly stained Htt positive cells are evident while a normal pattern of Nissl-stained neurons was retained. C, and insets below: Closer to the catheter track, Htt immunostaining was reduced to background levels while Nissl staining of neurons was retained.

an increase in striatal vulnerability in rats. Therefore, while WT-Htt plays a role in multiple cellular processes, including axonal transport, neuronal development, transcriptional regulation, and protection from cell death (Ross and Tabrizi, 2011), it is anticipated based on these studies that partial Htt lowering (of both WT and mutant Htt) in the adult may be both safe and effective. In the present study,

CED of an siRNA targeting both wild-type and mutant Htt was well-tolerated for up to 28 days and resulted in no more than 75% lowering of Htt mRNA in any single punch, and approximately 45% suppression of Htt mRNA on average throughout most of the NHP striatum. This level of Htt mRNA reduction corresponded to approximately 32% reduction of Htt protein by semi-quantitative Western blot analysis. Although there was apparently a more pronounced attenuation of immunostaining intensity, this is likely due to different sensitivities of the immunohistochemical and Western blot methods. Partial reduction of Htt as observed in the present study may be sufficient to provide clinical benefit, based on the reported effects of RNAi in rodent models.

A key aspect of understanding drug delivery is the relationship of local tissue concentration to drug activity. In the present study, a threshold siRNA level of 0.65 mg_{siHtt}/g_{tissue} was found to be required for Htt suppression by 45%. This threshold siRNA concentration, together with quantitative autoradiographic data at different infusion rates and concentrations of siRNA, was then used to generate a model of volume of effective suppression – the tissue volume over which this threshold siRNA concentration is attained – as a function of these two input parameters, infusion rate and concentration of siRNA. This response model revealed that both input parameters have a nearly equal effect on $V_{s,Str}$, and that there is an interaction effect of the 2 parameters on V_s. The equations for V_s and $V_{s,Str}$ differ primarily due to anatomical considerations. The asymmetrical, oblong shape of the striatum, in contrast to the spherical shape of siRNA distribution, results in a lesser impact of infusion rate and concentration of infusate on volume of suppression within the striatum ($V_{s,Str}$) than within the entire brain (V_s). This finding has important implications for optimizing catheter configuration, including catheter placement and use of multiple catheters, to achieve maximal siRNA distribution within the striatum, while using minimal quantities of infused siRNA.

A critical challenge for clinical translation of local CNS delivery is the scalability of drug distribution and effect. Unilateral putamenal volumes in early stage Huntington's disease patients have been reported to be 2.2 ± 0.6 (Rosas et al., 2001) or $2.7 \pm 0.6\ cm^3$ (Vandenberghe et al., 2009) on average, as determined by MRI morphometry studies, approximately 3-fold greater than that in rhesus monkey (Matochik et al., 2000). The response models of V_s in rhesus monkeys, generated in the present study, provide the experimental foundation for future development of a precise computational model to predict V_s in the specific targeted anatomy in the Huntington's disease brain, using different dosing paradigms, and numbers and placement of catheters, as well as incorporating patient-to-patient variation in shape and size of the striatum. A further consideration is that therapy in Huntington's disease patients should ultimately provide bilateral treatment of the cortex, in addition to the striatum. In order to achieve drug distribution in the cortex and striatum of both hemispheres, multiple catheters will be needed. Further technological development of intraparenchymal infusion systems may be required to achieve this.

In summary, we have shown here the translational potential of local CNS administration of siRNA therapeutics using CED for the treatment of CNS disorders. This method of siRNA delivery provides distribution of drug and resultant gene silencing across large regions of the nonhuman primate brain, indicating that the approach is scalable for coverage of significant regions of the human brain. In CNS disorders such as Huntington's disease, where suppression of a pathogenic gene in a critical anatomical region is likely to have significant clinical benefit, local CNS administration of RNAi therapeutics with CED has the potential to provide an important disease-modifying therapeutic strategy. Further, longer-term studies are warranted to investigate the feasibility of this approach for treating Huntington's disease.

Supplementary materials related to this article can be found online at doi: 10.1016/j.expneurol.2011.11.020.

Acknowledgments

The research was supported by grants from Alnylam Pharmaceuticals and Medtronic Neuromodulation, and some of the authors are employees and shareholders of these companies. We thank Lauren Lesser and Maryellen Livingston for graphics assistance, and Mike Kaytor and QPS Pharmaceutical Services for technical assistance.

References

Ai, Y., Markesbery, W., Zhang, Z., Grondin, R., Elseberry, D., Gerhardt, G.A., Gash, D.M., 2003. Intraputamenal infusion in aging rhesus monkeys: distribution and dopaminergic effects. J. Comp. Neurol. 461, 250–261.

Bobo, R.H., Laske, D.W., Akbasak, A., Morrison, P.F., Oldfield, E.H., Dedrick, R.L., 1994. Convection-enhanced delivery of macromolecules in the brain. Proc. Natl. Acad. Sci. U.S.A. 91, 2076–2080.

Bogdahn, U., Hau, P., Stockhammer, G., Venkataramana, N.K., Mahapatra, A.K., Suri, A., Balasubramaniam, A., Nair, S., Oliushine, V., Parfenov, V., Poverennova, I., Zaaroor, M., Jachimczak, P., Ludwig, S., Schmaus, S., Heinrichs, H., Schlingensiepen, K.H., 2011. Targeted therapy for high-grade glioma with the TGF-Beta2 inhibitor Trabedersen: results of a randomized and controlled phase IIb study. Neuro Oncol. 13, 132–142.

Boudreau, R.L., McBride, J.L., Martins, I., Shen, S., Xing, Y., Carter, B.J., Davidson, B.L., 2009. Nonallele-specific silencing of mutant and wild-type huntingtin demonstrates therapeutic efficacy in Huntington's disease mice. Mol. Ther. 17, 1053–1063.

DiFiglia, M., Sena-Esteves, M., Chase, K., Sapp, E., Pfister, E., Sass, M., Yoder, J., Reeves, P., Pandey, R.K., Rajeev, K.G., Manoharan, M., Sah, D.W., Zamore, P.D., Aronin, N., 2007. Therapeutic silencing of mutant huntingtin with siRNA attenuates striatal and cortical neuropathology and behavioral deficits. Proc. Natl. Acad. Sci. U.S.A. 104, 17204–17209.

Drouet, V., Perrin, V., Hassig, R., Dufour, N., Auregan, G., Alves, S., Bonvento, G., Brouillet, E., Luthi-Carter, R., Hantrave, P., Deglon, N., 2009. Sustained effects of nonallele-specific Huntingtin silencing. Ann. Neurol. 65, 276–285.

Fiandaca, M.S., Varenika, V., Eberling, J., McKnight, T., Bringas, T., Pivirotto, P., Beyer, J., Hadaczek, P., Bowers, W., Park, J., Federoff, H., Forsaueth, J., Bankiewicz, K.S., 2009. Real-time MR imaging of adeno-associated viral vector delivery to the primate brain. Neuroimage 47 (Suppl 2), 27–35.

Ge, P., Querbes, W., Chen, Q., Tan, P., Hadwiger, P., John, M., Solomon, M., Costigan, J., Wang, G., Fan, Y., Maier, M., Charisse, K., Nechev, L., Vornlocher, H., Adams, M., Kaemmerer, W., Gwost, D., Manoharan, M., Kotelianski, V., Bumcrot, D., Sah, D.W.Y., 2009. Developing RNAi therapeutics targeting huntingtin with local CNS delivery: in vitro and rat studies. Society for Neuroscience Program No. 433.3, Online.

Grondin, R., Zhang, Z., Elsberry, D., Gerhardt, G.A., Gash, D.M., 2001. Chronic intracerebral delivery of trophic factors via a programmable pump as a treatment for parkinsonism. In: Mouradian, M.M. (Ed.), Parkinson's Disease—Methods and Protocols. Humana Press, Totowa, New Jersey, pp. 257–267.

Groothuis, D.R., Ward, S., Itskovich, A.C., Dobrescu, C., Allen, C.V., Dills, C., Levy, R.M., 1999. Comparison of 14C-sucrose delivery to the brain by intravenous, intraventricular and convection-enhanced intracerebral infusion. J. Neurosurg. 90, 321–331.

Harper, S.Q., Staber, P.D., He, X., Eliason, S.L., Martins, I.H., Mao, Q., Yang, L., Kotin, R.M., Paulson, H.L., Davidson, B.L., 2005. RNA interference improves motor and neuropathological abnormalities in a Huntington's disease mouse model. Proc. Natl. Acad. Sci. U.S.A. 102, 5820–5825.

Heiss, J.D., Walbridge, S., Asthagiri, A.R., Lonser, R.R., 2010. Image-guided convection-enhanced delivery of muscimol to the primate brain. J. Neurosurg. 112, 790–795.

Kumar, P., Wu, H., McBride, J.L., June, K.E., Kim, M.H., Davison, B.L., Lee, S.K., Shankar, P., Manjunath, N., 2007. Transvascular delivery of small interfering RNA to the central nervous system. Nature 448, 39–43.

Lombardi, M.S., Jaspers, L., Spronkmans, C., Gellera, C., Taroni, F., DiMaria, E., Donato, S.D., Kaemmerer, W.F., 2009. A majority of Huntington's disease patients may be treatable by individualized allele-specific RNA interference. Exp. Neurol. 217, 312–319.

Lonser, R.R., Schiffman, R., Robison, R.A., Butman, J.A., Quezado, Z., Walker, M.L., Morrison, P.F., Walbridge, S., Murray, G.J., Park, D.M., Brady, R.O., Oldfield, E.H., 2007. Image-guided, direct convective delivery of glucocerebrosidase for neuronopathic Gaucher Disease. Neurology 68, 254–261.

Matochik, J.A., Chefer, S.I., Lane, M.A., Woolf, R.I., Morris, E.D., Ingram, D.K., Roth, G.S., London, E.D., 2000. Age related decline in striatal volume in monkeys as measured by magnetic resonance imaging. Neurobiol. Aging 21, 591–598.

Pfister, E.L., Kennington, L., Straubhaar, J., Waugh, S., Liu, W., Landwehrmeyer, B., DiFiglia, M., Vonsattel, J.P., Zamore, P.D., Aronin, N., 2009. Five siRNAs targeting three SNPs may provide therapy for three-quarters of Huntington's disease patients. Curr. Biol. 19, 774–778.

Rosas, H.D., Goodman, J., Chen, Y.I., Jenkins, B.G., Kennedy, D.N., Makris, N., Patti, M., Seidman, L.J., Beal, M.F., Koroshetz, W.J., 2001. Striatal volume loss in HD as measured by MRI and the influence of CAG repeat. Neurology 57, 1025–1028.

Ross, C.A., Tabrizi, S.J., 2011. Huntington's disease: from molecular pathogenesis to clinical treatment. Lancet Neurol. 10, 83–98.

Song, D.K., Lonser, R.R., 2008. Convection-enhanced delivery for the treatment of pediatric neurologic disorders. J. Child Neurol. 23, 1231–1237.

Thakker, D.R., Natt, F., Hüsken, D., Maier, R., Müllen, M., van der Putten, H., Hover, D., Cryan, J.F., 2004. Neurochemical and behavioral consequences of widespread gene knockdown in the adult mouse brain by using nonviral RNA interference. Proc. Natl. Acad. Sci. U.S.A. 101, 17270–17275.

The Huntington's Disease Collaborative Research Group, 1993. A novel gene containing a trinucleotide repeat that is expanded and unstable on Huntington's disease chromosomes. Cell 72, 971–983.

Vandenberghe, W., Demaerel, P., Dom, R., Maes, F., 2009. Diffusion-weighted versus volumetric imaging of the striatum in early symptomatic Huntington disease. J. Neurol. 256, 109–114.

Voges, J., Reszka, R., Gossmann, A., Dittmar, C., Richter, R., Garlip, G., Kracht, L., Coenen, H.H., Sturm, V., Wienhard, K., Heiss, W.D., Jacobs, A.H., 2003. Imaging-guided convection-enhanced delivery and gene therapy of glioblastoma. Ann. Neurol. 54, 479–487.

Walker, F.O., 2007. Huntington's disease. Lancet 369, 218–228.